Estuarine, Coastal and Shelf Science 335 (2026) 109842

Contents lists available at ScienceDirect

Estuarine, Coastal and Shelf Science

journal homepage: www.elsevier.com/locate/ecss

Typhoon-induced subsurface marine heatwaves in the South China Sea

Zhouhong Liu [a], Shukui Cheng [a], Anzhou Cao [a,*], Jinbao Song [a], Xinyu Guo [b]

[a] State Key Laboratory of Ocean Sensing & Ocean College, Zhejiang University, Zhoushan, China
[b] Center for Marine Environmental Studies, Ehime University, Matsuyama, Japan

ARTICLE INFO

Keywords:
Subsurface marine heatwaves
Typhoon
South China sea

ABSTRACT

Under global warming, the frequency and intensity of extreme events have significantly increased, exerting dramatic impacts on the natural ecosystems and human society. We report that typhoons, as extreme weather events, can trigger subsurface marine heatwaves (MHWs), which are extreme ocean events. Based on 27-year ocean reanalysis data, a total of 9 typhoon-induced subsurface MHW events are identified in the South China Sea, with most of them occurring in the nearshore shallow waters. The enhanced mixing induced by the typhoon, relatively high subsurface temperature percentile prior to the typhoon, and sufficiently long duration of subsurface warming are three key factors for typhoon-induced subsurface MHWs. Although the occurring probability of typhoon-induced subsurface MHW events is relatively low, the co-occurrence of such extreme events poses a serious threat to the marine environment and requires special attention.

1. Introduction

Under global warming, both the frequency and intensity of extreme events have increased substantially over recent decades and are projected to be further exacerbated (Frölicher et al., 2018; Oliver et al., 2018; Cheng et al., 2019; IPCC et al., 2022), exerting dramatic impacts on the natural ecosystems and human society (Smale et al., 2019; Gruber et al., 2021; Liu et al., 2025). As a vital component of Earth's ecosystems, the ocean has absorbed more than 90% of the excess heat resulting from global warming and plays a crucial role in modulating the high-frequency climate variability (Cheng et al., 2019; IPCC et al., 2021). The ocean supplies energy for numerous extreme events (Emanuel, 2005; Frölicher et al., 2018; Balaguru et al., 2022), many of which originate and develop within the marine environments. These extreme events, in turn, alter the oceanic conditions (Price, 1981; Lin et al., 2008; Muis et al., 2016), potentially leading to severe disasters. Therefore, understanding the drivers and impacts of such extreme events is of great importance.

As one of these extreme events, marine heatwaves (MHWs) exert devastating impacts on the marine ecosystems, yielding coral bleaching, extensive algal degradation and mass mortality of coastal fish (Pearce and Feng, 2013; Wernberg et al., 2013; Bond et al., 2015; Guibourd de Luzinais et al., 2024). MHWs can either be confined to shallow waters or extend to deep layers (Schaeffer and Roughan, 2017; Holbrook et al., 2019; Schaeffer et al., 2023; Sun et al., 2023; Zhang et al., 2023b; Köhn et al., 2024). They are driven by oceanic and atmospheric processes including air-sea heat fluxes, ocean advection or mixing (Holbrook et al., 2019; Amaya et al., 2021; Schaeffer et al., 2023). The generation and evolution of MHWs are also influenced by the regional ocean environment, including ocean dynamics and the local bathymetry (Zhang et al., 2023b; Capotondi et al., 2024). Previous studies have indicated that there is no clear correlation between the subsurface and surface MHWs (Hu et al., 2021; Sun et al., 2023). Surface MHWs have been widely studied based on the satellite-observed sea surface temperature (SST) data (e.g. Bond et al., 2015; Frölicher et al., 2018; Holbrook et al., 2019; Smale et al., 2019; Guibourd de Luzinais et al., 2024; Zhou et al., 2025), while the understanding of subsurface MHWs remains limited due to the sparse subsurface temperature observations (Hu et al., 2021; He et al., 2024). Thus, investigating the mechanisms of subsurface MHWs is crucial.

Typhoons are another form of extreme events, commonly causing severe environmental disruption and economic losses. During their formation and intensification, typhoons derive vast amounts of heat and moisture from the ocean, while simultaneously inputting energy into it. This energy significantly triggers mixing within the mixed layer (He and Chen, 2011; Zhang et al., 2021). Furthermore, a portion of this energy can propagate into the deep ocean via near-inertial waves (e.g. Cao et al., 2018; Raja et al., 2022), thereby enhancing the mixing in the ocean interior (Polton et al., 2008; Zhang et al., 2016; Qiao et al., 2022). In turn, the intense mixing induced by typhoons results in dramatic

* Corresponding author.
E-mail address: caoanzhou@zju.edu.cn (A. Cao).

https://doi.org/10.1016/j.ecss.2026.109842
Received 31 December 2025; Received in revised form 24 February 2026; Accepted 18 March 2026
Available online 19 March 2026

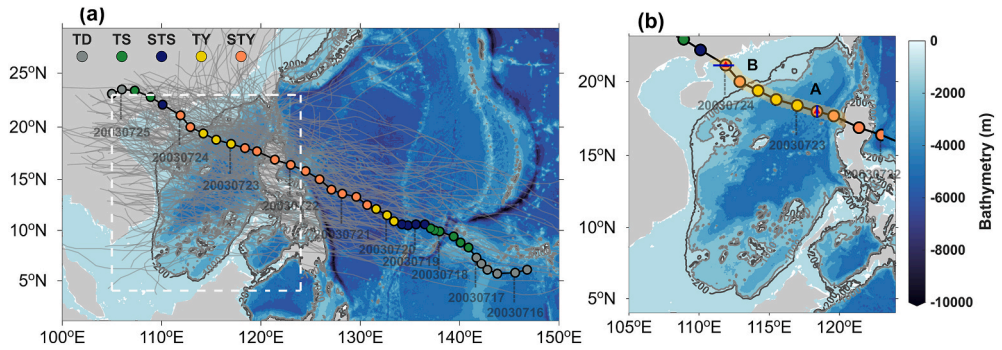

Fig. 1. Bathymetry and typhoon tracks. (a) Tracks of all the typhoons entering the SCS during 1993-2020 (gray curves). The black curve is the track of Typhoon Imbudo (2003) and the colored dots denote its statuses (TD: tropical depression; TS: tropical storm; STS: severe tropical storm; TY: typhoon; STY: severe typhoon). The white dashed box denotes the study domain, and the blue shadings indicate the bathymetry. (b) Track of Typhoon Imbudo (2003) in the SCS. The light-yellow shadings indicate the typhoon's influencing region (within 50 km of the typhoon track). The red triangles and blue lines denote the two points (point A: 18.00°N, 118.40°E; point B: 21.10°N, 111.90°E) and two sections (section A: a meridional section through point A; section B: a zonal section through point B) selected for analysis. (For interpretation of the references to color in this figure legend, the reader is referred to the Web version of this article.)

temperature variations in the ocean (Price, 1981; Zhao et al., 2017; Zhang et al., 2021; Zhang, 2023; Cheng et al., 2024). Based on the heat pump hypothesis (Emanuel, 2001; Zhang et al., 2016), the typhoon-induced mixing can cause SST cooling and subsurface warming, with the maximum temperature variation occurring at the base of the mixed layer or deeper layers (Price, 1981; Jacob et al., 2000; Zhang et al., 2016; Liu et al., 2022; Cheng et al., 2024; Han et al., 2024). Meanwhile, the thermal response of the upper ocean to typhoons is modulated by the deepening of the surface mixed layer (Zhang et al., 2016; Zhang, 2023; Cheng et al., 2024), which is influenced by both the ocean stratification and typhoon characteristics (such as the maximum wind speed, radius of the maximum wind speed, translation speed and track). An increase in the radius of the maximum wind speed and a decrease in the translation speed can prolong the duration of a typhoon at a given point, typically resulting in a deeper mixed layer depth (MLD) and stronger SST cooling (Pun et al., 2018; Liu et al., 2023), whereas the subsurface warming remains uncertain (Park et al., 2011; Vincent et al., 2013). After the passage of the typhoon, the SST is gradually recovered to the pre-typhoon level, whereas the subsurface warming may persist for a long duration, resulting in an increase in the net ocean heat content (Park et al., 2011; Cheng et al., 2015; Zhang et al., 2016, 2023a; Hsu and Ho, 2019; Qiao et al., 2022).

Because typhoons can induce sustained subsurface warming, we speculate that they are a possible driver of subsurface MHWs. This speculation is potentially supported by the underwater glider observation of Zhang et al. (2024), who documented six days of persistent warming after the passage of Typhoon Mangkut (2018) in the nearshore shallow waters of the South China Sea (SCS). According to Hobday et al. (2016), an MHW is a thermal event with associated temperature exceeding the 90th percentile threshold for at least 5 days. Therefore, if typhoon-induced subsurface warming meets this criterion, subsurface MHWs occur. In light of this, we conduct a systematic investigation of subsurface MHWs in the SCS from 1993 to 2020 using ocean reanalysis data, with a particular focus on their relationship with typhoon activities.

2. Data and methods

2.1. Typhoon best-track data and bathymetry data

The typhoon best-track data utilized in this study were downloaded from the China Meteorological Administration (https://tcdata.typhoon.org.cn/zjljsjj.html; Ying et al., 2014; Lu et al., 2021), encompassing the tracks and intensities of typhoons in the Northwestern Pacific Ocean since 1949. In this study, a total of 260 typhoons that passed over the SCS from 1993 to 2020 were taken into consideration, of which the tracks are illustrated in Fig. 1a. The bathymetry data were obtained from the National Oceanic and Atmospheric Administration (NOAA) ETOPO2022 global relief model data (https://www.ncei.noaa.gov/products/etopo-global-relief-model; NOAA National Centers for Environmental Information, 2022), which are also shown in Fig. 1a.

2.2. Temperature, salinity and velocity data

The daily mean water potential temperature, salinity and velocity data of the Global Ocean Reanalysis and Simulations (GLORYS) 12V1 products (https://data.marine.copernicus.eu/product/GLOBAL_MULTIYEAR_PHY_001_030/download; Jean-Michel et al., 2021) were obtained from the current real-time global forecasting system of Copernicus Marine Environmental Monitoring Service (CMEMS). These data have a horizontal resolution of 1/12° and consist of 50 vertical layers, covering the period from January 1, 1993 to June 30, 2021. The reanalysis uses the Nucleus for European Modeling of the Ocean (NEMO) ocean model, which is driven at the surface by the European Center for Medium-Range Weather Forecasts reanalysis data. The GLORYS12V1 products have been validated by in situ observations, demonstrating their excellent performance in reproducing variations in the ocean temperature and MLD, and have been widely used in studies of subsurface MHWs (e.g. Amaya et al., 2023; Sun et al., 2023; Guo et al., 2024). Hence, we utilized these data at 0-500 m depth (layers 1-31) to study the subsurface MHWs in the SCS.

2.3. MHW identification

Based on the definition of Hobday et al. (2016), a MHW is a thermal event with associated temperature exceeding the 90th percentile threshold for at least 5 days, with any dips below this threshold lasting two days or less being ignored; The short-term temperature exceedances that do not meet the five-day criterion are classified as marine heat spikes (MHSs). Using the daily temperature within an 11-day window centered on each date, the 90th percentile threshold and climatological mean of temperature at each layer were calculated for the period 1993-2020 (Hobday et al., 2016). This approach allowed us to derive the daily occurrence of MHWs at all the depths in the SCS. The MHW detection code was provided by (Zhao and Marin, 2019).

2.4. Determination of typhoon-induced subsurface MHW events

We focused on the MHWs occurring between the MLD and 500 m depth, within 50 km of the typhoon track, and within a 10-day window following each typhoon's passage. The MLD is defined as the depth at which the potential density difference relative to the potential density at

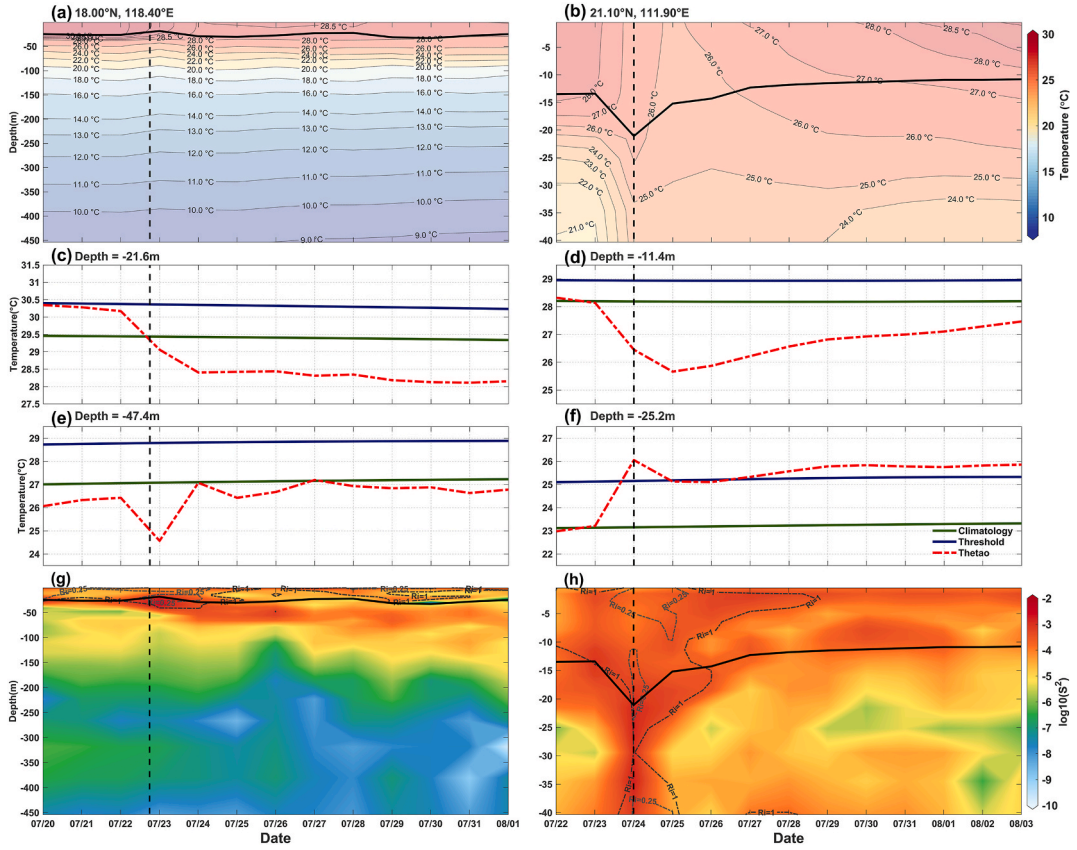

Fig. 2. Upper-ocean temperature variations induced by Typhoon Imbudo (2003). Upper-ocean temperature (shadings) at Points (a, c and e) A and (b, d and f) B. Upper-ocean shear squared (shadings) and gradient Richardson number (gray dashed contours) at Points (g) A and (h) B. In (a, b, g and h), the black curve denotes the MLD. In (c-f), the green solid curve denotes the temperature climatology, the blue solid curve denotes the 90th percentile threshold, and the red dash-dotted curve is the raw temperature. In each subfigure, the vertical dashed line denotes the time when Typhoon Imbudo passed over the corresponding point. (For interpretation of the references to color in this figure legend, the reader is referred to the Web version of this article.)

10 m is 0.125 kg/m^3 (Monterey and Levitus, 1997). As the aim of this study is to explore the subsurface MHWs induced by typhoons, those caused by other mechanisms were excluded from our analysis. After excluding the subsurface MHWs prior to typhoons and removing the subsurface MHWs associated with mesoscale eddies (e.g. Bian et al., 2023; He et al., 2024), we obtained the subsurface MHW events potentially triggered by typhoons. It is noteworthy that in all these typhoon-triggered events, no subsurface MHWs were observed prior to the typhoon's arrival.

2.5. Gradient richardson number

Typhoons transfer momentum into the ocean, which is an important source of mixing in the ocean. However, the GLORYS12V1 products cannot be directly used to estimate the mixing. Therefore, the gradient Richardson number was calculated to approximately represent the intensity of mixing:

$$\mathrm{Ri} = N^2 \Big/ S^2 = \left(-\frac{g}{\rho_0}\frac{d\rho}{dz} \right) \Big/ \left[\left(\frac{\partial u}{\partial x}\right)^2 + \left(\frac{\partial v}{\partial y}\right)^2 \right] \quad (1)$$

where N is the buoyancy frequency, S is velocity shear, g is the acceleration of gravity, ρ is the density, ρ_0 is the reference density, u and v are the zonal and meridional velocity components, and x, y, and z are the zonal, meridional, and vertical coordinates, respectively. Shear instability is conventionally identified by the criterion Ri < 0.25. However, for the real ocean conditions, Dmitrenko et al. (2012) proposed a more lenient criterion, suggesting that shear instability can occur when Ri < 1.

3. Results

3.1. Subsurface MHW induced by Typhoon Imbudo (2003)

In this section, the subsurface MHW induced by Typhoon Imbudo (2003) is shown as an example. Typhoon Imbudo was the 7th typhoon in 2003, which was generated in the equatorial Pacific and moved northwestward (Fig. 1a). In the Philippine Sea, it was strengthened to a severe typhoon. After passing over the Luzon Island, it was slightly weakened to a typhoon and then re-strengthened to a severe typhoon before landing, resulting in great infrastructure damage and economic losses (Li et al., 2005). Typhoon Imbudo induced significant SST cooling in the SCS, with a maximum cooling of −3.50 °C (Fig. S1 in the supplementary material). Accompanied by the passage of Typhoon Imbudo, significant warming was found below the mixed layer in the nearshore shallow waters, ultimately leading to the formation of a subsurface MHW; In the deep waters of the SCS Basin, Typhoon Imbudo also caused subsurface warming, but the temperature did not exceed the 90th percentile threshold, failing to form a subsurface MHW (Fig. 2).

The subsurface warming induced by Typhoon Imbudo exhibited differences in the shallow (<200 m) and deep (>200 m) waters. We selected two points (point A: 18.00°N, 118.40°E; point B: 21.10°N, 111.90°E) as examples to show the temperature differences between the shallow and deep waters. It should be noted that Typhoon Imbudo maintained its status as a severe typhoon at both points (Fig. 1b), and before Typhoon Imbudo entered the SCS, no subsurface MHW was detected near either point. After the passage of Typhoon Imbudo, the thickness of MLD at point A was first deepened and subsequently recovered (Fig. 2a) and the temperature in the MLD was significantly

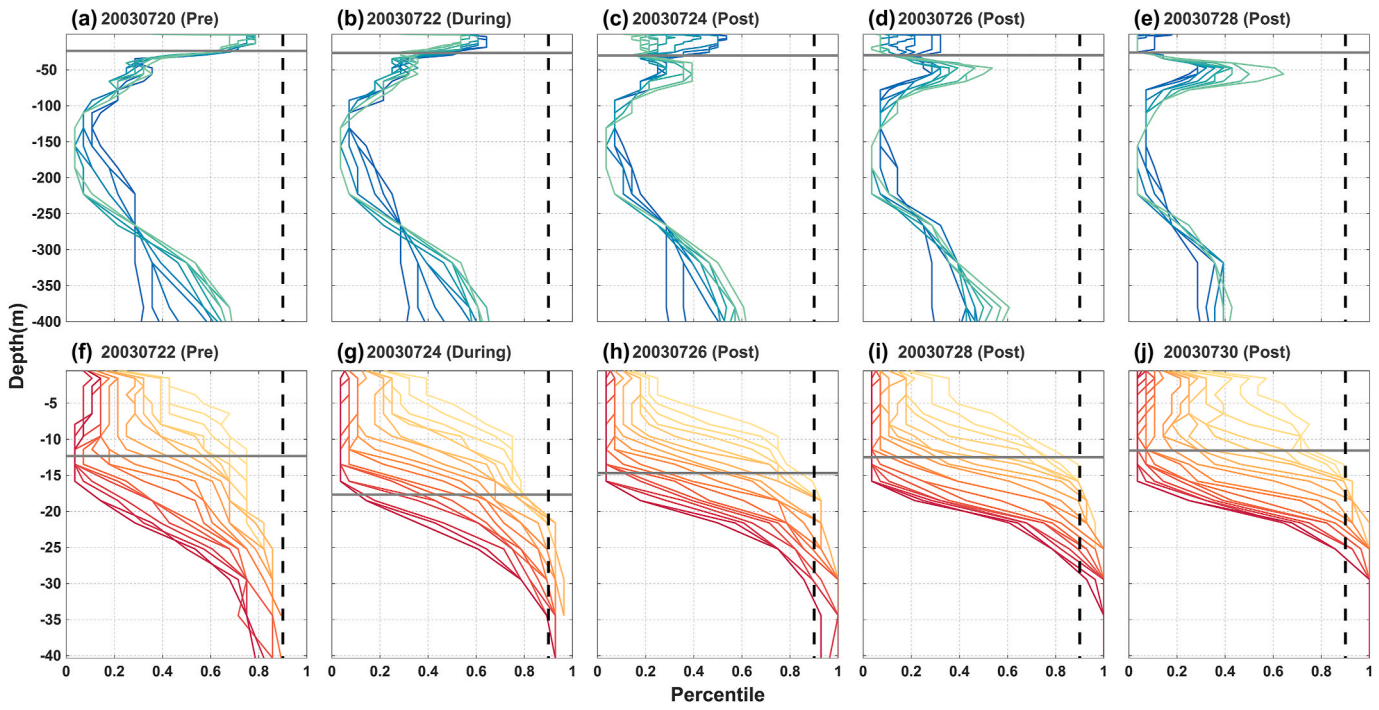

Fig. 3. Variations of temperature percentiles during Typhoon Imbudo (2003). Temperature percentiles at grids along section (a-e) A and (f-j) B during the passage of Typhoon Imbudo. In each subfigure, the horizontal gray solid line indicates the averaged MLD along the section, and the vertical black dashed line denotes the 90th percentile.

cooled (Fig. 2a and c). Within the thin layer beneath the MLD, a temperature increase was found after an initial cooling, and the maximum temperature increase occurred on July 27, 2003, five days after the passage of Typhoon Imbudo (Fig. 2a and e). However, this warming only reached the temperature climatology criterion, failing to form a MHS. The situation at point B was different. After the passage of Typhoon Imbudo, the water column was rapidly mixed, causing a pronounced cooling in the mixed layer and warming below the MLD (Fig. 2b). On August 3, 2003, 10 days after the passage of Typhoon Imbudo, the temperature in the mixed layer was not fully recovered to the status prior to the typhoon (Fig. 2b and d), and the temperature below the MLD remained significantly higher than its pre-typhoon level (Fig. 2b and f). As shown in Fig. 2f, a pronounced warming (>2 °C) was observed at the depth of 25.2 m and lasted for 10 days (from 24 July to August 3, 2003). At the same time, this warming exceeded the 90th percentile threshold for more than five consecutive days (Fig. 2f), marking the occurrence of a subsurface MHW. The occurrence of such subsurface MHW was largely attributed to the enhanced mixing caused by Typhoon Imbudo (Fig. 2h). It should be noted that Typhoon Imbudo also caused intense mixing at point A (Fig. 2g). However, the mixing here merely elevated the subsurface temperature within 1 °C, failing to reach the 90th percentile threshold (Fig. 2e).

Given that the extreme temperature at a single point might have bias, we further examined the temperature variations along sections A and B. Section A is the meridional section through point A and section B is the zonal section through point B, both of which are within the typhoon's influencing region (Fig. 1b). Fig. 3 illustrates the variations of temperature percentiles along the two sections. Prior to the typhoon's arrival, the temperature percentiles along section A exhibited a concave pattern, initially decreasing with depth before subsequently increasing (Fig. 3a). During the passage of the typhoon, the temperature percentiles in the mixed layer decreased rapidly and those in the subsurface layer were apparently increased (Fig. 3b–e), consistent with typhoon-induced SST cooling and subsurface warming (Fig. 2a and Fig. S2 in the supplementary material). Although the temperature percentiles in the subsurface layer were increased by Typhoon Imbudo, none of them exceeded the 90th percentile (Fig. 3b–e), indicating that no subsurface MHW occurred here. In contrast, the temperature percentiles along

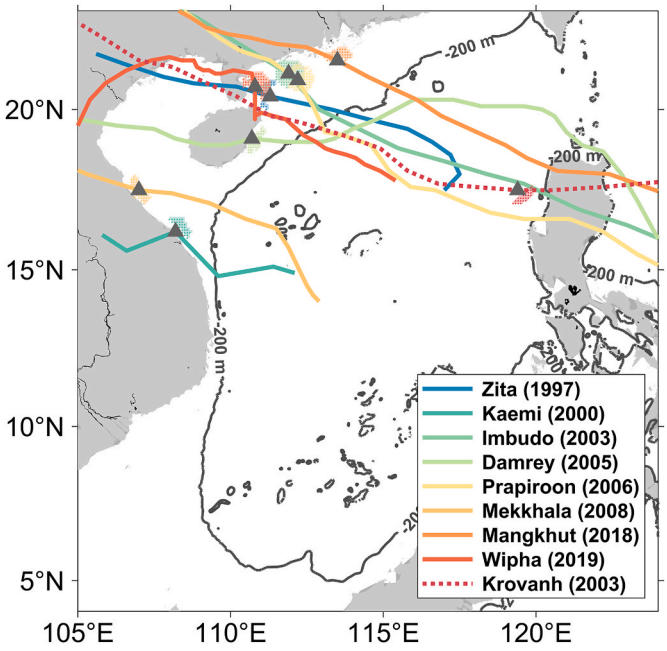

Fig. 4. Statistics of typhoon-induced subsurface MHW events in the SCS from 1993 to 2020. The solid (dotted) curves denote the typhoons that induced subsurface MHWs in the shallow (deep) waters of the SCS. The triangles indicate the minimal analytical unit for quantifying the relation between typhoons and subsurface MHWs, which are similar to point B in Fig. 1b. The shading areas represent the spatial regions of subsurface MHWs induced by the corresponding typhoon marked by the same color. (For interpretation of the references to color in this figure legend, the reader is referred to the Web version of this article.)

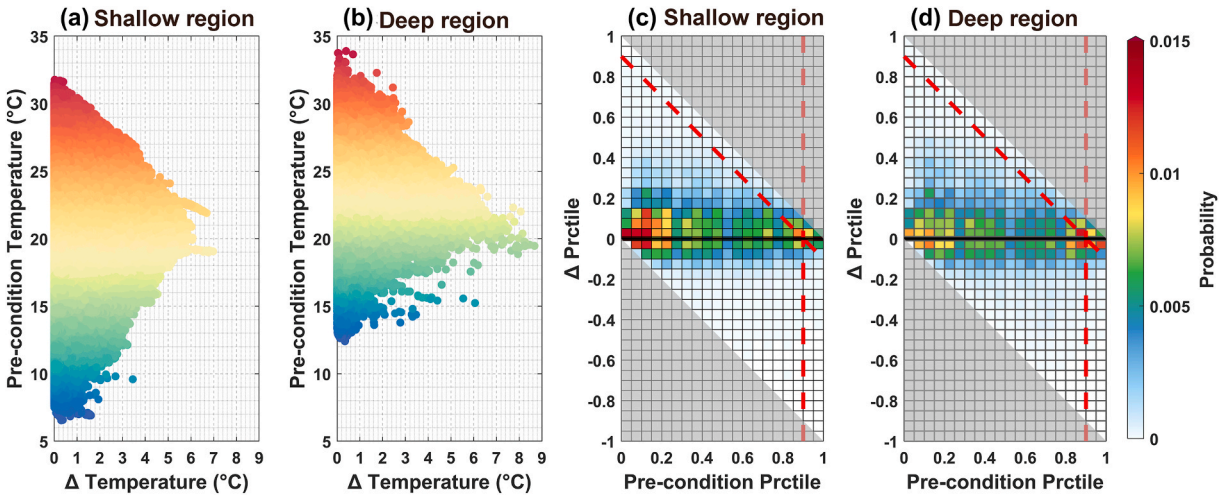

Fig. 5. Typhoon-induced temperature and percentile variations in the upper SCS. Typhoon-induced temperature warming versus pre-condition temperature before the typhoon in the (a) deep and (b) shallow waters in the SCS. Probability distributions of typhoon-induced temperature percentile variations versus pre-condition temperature percentile before the typhoon in the (c) deep and (d) shallow waters in the SCS. In (c and d), the vertical red dashed line denotes the 90th temperature percentile before the typhoon and the inclined one denotes the 90th temperature percentile after the typhoon. The gray shadings indicate impossible cases. (For interpretation of the references to color in this figure legend, the reader is referred to the Web version of this article.)

section B prior to the typhoon's arrival were at a relatively high level (Fig. 3f), but they did not reach the criterion of MHWs. With the passage of the typhoon, the water column was rapidly mixed (Fig. S3 in the supplementary material). The temperature percentiles almost remained invariant in the mixed layer, but were significantly elevated below the MLD, obviously exceeding the 90th percentile (Fig. 3g–j). These results confirm that Typhoon Imbudo caused a coherent subsurface MHW in the shallow waters on the continental shelf of the SCS.

3.2. Statistics of typhoon-induced subsurface MHWs in the SCS from 1993 to 2020

The occurrence of the subsurface MHW triggered by Typhoon Imbudo (2003) was not an isolated event. Our analysis revealed a total of 9 typhoon-induced subsurface MHW events in the SCS from 1993 to 2020, which are shown in Fig. 4 and Table S1 in the supplementary material. Specifically, Typhoon Mangkut (2018), which has been reported to cause significant subsurface warming (Zhang et al., 2024), also induced a subsurface MHW. Moreover, typhoon-induced subsurface MHWs mainly occurred in the nearshore shallow waters of the SCS. In the deep waters of the SCS Basin, there was only one MHW event caused by Typhoon Krovanh (2003). Further analysis showed that for most of the typhoon-induced subsurface MHW events, the subsurface temperature percentile prior to the typhoon's arrival was already relatively high, which provides favorable conditions for the formation of subsurface MHWs via typhoon-induced heat pumping (Figs. S4-S11 in the supplementary material).

3.3. Key factors of typhoon-induced subsurface MHW events

The first key factor is the enhanced mixing induced by the typhoon, which governs the temperature variations in the upper ocean (Price, 1981; Emanuel, 2001; Pei et al., 2015; Zhang et al., 2016; Cheng et al., 2024). The mixing causes downward intrusion of surface warm water and hence warms the subsurface water (Zhang et al., 2016, 2024; Hsu and Ho, 2019). As shown in Fig. 5a and b, the maximum subsurface warming induced by typhoons exceeds 6 °C in the deep waters and 8 °C in the shallow waters in the SCS. The subsurface warming further increases the subsurface temperature percentile, serving as a crucial factor for subsurface MHWs.

The relatively high subsurface temperature percentile prior to the typhoon is also important for the formation of subsurface MHWs. Fig. 5c and d displays the probabilities of subsurface temperature percentiles before and after the passage of typhoons in the deep and shallow waters in the SCS. The vertical red dashed line denotes the 90th temperature percentile before the typhoon and the inclined one denotes the 90th temperature percentile after the typhoon. Typhoon-induced subsurface MHWs can only occur in the top-left quadrant formed by these two lines. However, this is a necessary but not sufficient condition, as the duration for which the temperature percentile exceeds 90% has not been considered. In other words, the top-left quadrant formed by the two red dashed lines includes both the occurrence probabilities of typhoon-induced subsurface MHWs and MHSs. Nevertheless, in the top-left quadrant formed by the two red dashed lines, larger probabilities mainly appear with relatively high temperature percentile prior to the typhoon, demonstrating that it is an important factor for subsurface MHWs and MHSs in both the shallow and deep waters in the SCS.

Sufficiently long duration of subsurface warming is also necessary according to the definition of MHWs (Hobday et al., 2016). Actually, the differences in the duration of subsurface warming between the deep and shallow waters of the SCS lead to the different occurring probabilities of subsurface MHWs. According to Fig. 5c and d, the total probability in the top-left quadrant formed by the two red dashed lines is 3.22% in the deep waters and 3.18% in the shallow waters, which are comparable. However, in the 9 typhoon-induced subsurface MHW events in the SCS (Fig. 4), only one occurred in the deep waters whereas all the others occurred in the shallow waters.

In summary, the occurrence of typhoon-induced subsurface MHWs is attributed to a combination of enhanced mixing, relatively high subsurface temperature percentile and sufficiently long duration of subsurface warming. Moreover, the contributions of these factors may vary, driven by the differences in typhoon characteristics and oceanic conditions. Consequently, 9 typhoon-induced subsurface MHW events were identified in the SCS between 1993 and 2020, with most occurring in the nearshore shallow waters.

4. Summary and discussion

Although typhoons are found to suppress surface MHWs (Pun et al., 2025), we reveal in this study that they can trigger subsurface MHWs. From 1993 to 2020, a total of 9 typhoon-induced subsurface MHW events were identified in the SCS based on the GLORYS12V1 ocean

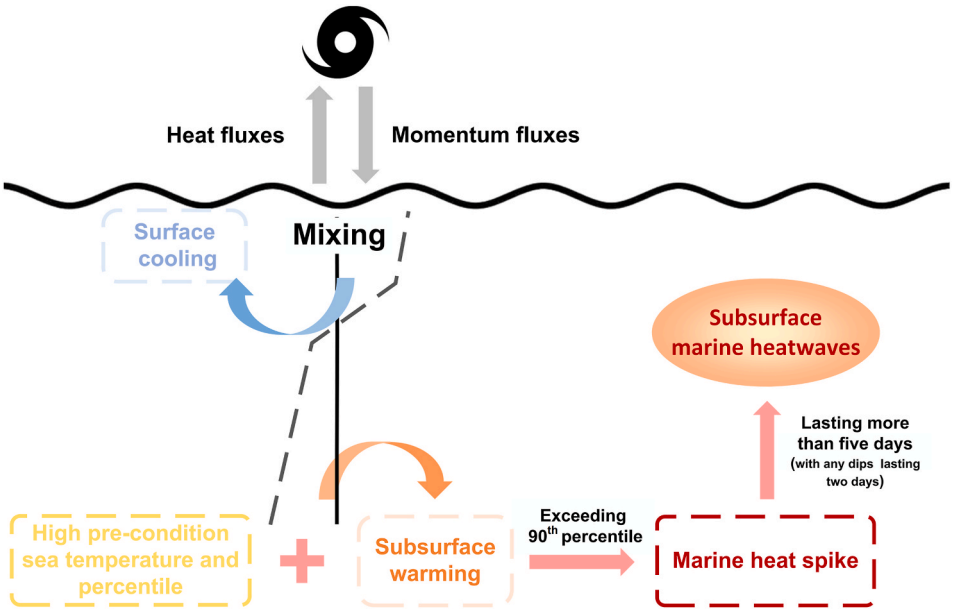

Fig. 6. Schematic diagram for typhoon-induced subsurface MHWs. The gray dashed curve denotes the pre-typhoon temperature, and the black solid line denotes the temperature of the homogenized mixed water column after the typhoon.

reanalysis data. Such events were characterized by a relatively high pre-typhoon temperature percentile in the ocean, followed by a substantial and prolonged increase of subsurface temperature, with typhoon-induced mixing playing a key role in the process. Fig. 6 summarizes the mechanism of typhoon-induced subsurface MHWs.

Results of this study also indicate that typhoons are more likely to trigger subsurface MHWs in shallow waters than in deep waters (Fig. 4), whereas the probabilities of inducing MHSs is nearly identical in both regimes (Fig. 5). The reason is that shallow waters provide more favorable conditions for the evolution from MHSs into MHWs, compared to deep waters. First, the limited depth of shallow waters inhibits vertical heat advection and diffusion. Consequently, typhoon-induced subsurface warming becomes trapped, favoring the formation of subsurface MHWs. Second, typhoons can easily disrupt the stratification in shallow waters, promoting homogenized mixing and enhancing subsurface warming. Third, the well-mixed water column efficiently absorbs solar radiation and rapidly transports heat from the surface to subsurface layers, further amplifying subsurface warming. Collectively, these processes delay the recovery of SST and prolong the subsurface warming induced by typhoons (Dzwonkowski et al., 2020), ultimately facilitating the development of subsurface MHWs. In contrast, the much thicker column of deep waters facilitates vertical heat advection and diffusion, which can transport typhoon-induced subsurface warming to deeper layers. Moreover, the typically strong stratification in deep waters is resistant to complete breakdown by the typhoon, thereby limiting the potential for sustained subsurface warming. Consequently, in deep waters, typhoon-induced subsurface warming typically lacks the persistence required to meet the MHW duration criterion (Hobday et al., 2016).

Although this study specifically focuses on the typhoon-induced subsurface MHWs in the SCS, such events are also likely to occur in other shallow oceans subject to frequent typhoon activities. For example, Typhoon Lingling (2019) caused a subsurface MHW near the western coast of the Korean Peninsula (Fig. S12 in the Supplementary Material). Moreover, typhoon-induced subsurface MHWs exhibit little dependence on the background climate variability. All the 9 events identified in this study (Fig. 4) occurred during the typhoon peak season from July to October (Table S1 in the Supplementary Material), and the subsurface warming remains significant even after removing the seasonal cycle. Moreover, no statistically significant correlation is found between these subsurface MHW events and the Niño 3.4 index (Fig. S13 in the Supplementary Material), suggesting a weak link to the large-scale interannual variability. This independence can be attributed to the fact that typhoons drive rapid oceanic responses on timescales much shorter than those of background climate modes, minimizing the modulating effects from slower climate variabilities.

Typhoons and MHWs are extreme weather and ocean events, respectively, each of which has profound impacts on the marine ecosystems and marine engineering (Hongo et al., 2012; Thomson et al., 2014; Long et al., 2016; Anticamara and Go, 2017; Frölicher and Laufkötter, 2018; Gruber et al., 2021; Capotondi et al., 2024). Thus, the co-occurrence of typhoons and subsurface MHWs can be regarded as compound extreme events (Zscheischler and Seneviratne, 2017; Zscheischler et al., 2018; Zhou et al., 2025). Such events may exacerbate the impacts on temperature-sensitive ecosystems, leading to phenomena like coral bleaching and hypoxia (Dzwonkowski et al., 2020). Although the occurring probability of typhoon-induced subsurface MHWs is relatively low in the existing reanalysis data, it remains unclear whether this will change, especially under global warming. Therefore, gaining deeper insight into how such compound extreme events occur is crucial for improving forecasts and mitigating their extreme consequences. Such knowledge is also vital for enabling managers and policymakers to develop proactive strategies.

CRediT authorship contribution statement

Zhouhong Liu: Data curation, Formal analysis, Investigation, Methodology, Software, Visualization, Writing – original draft, Writing – review & editing. **Shukui Cheng:** Writing – review & editing. **Anzhou Cao:** Conceptualization, Methodology, Supervision, Writing – original draft, Writing – review & editing. **Jinbao Song:** Supervision, Writing – review & editing. **Xinyu Guo:** Supervision, Writing – review & editing.

Declaration of competing interest

The authors declare that they have no known competing financial interests or personal relationships that could have appeared to influence the work reported in this paper.

Acknowledgements

This study is supported by the Zhejiang Provincial Natural Science Foundation of China under Grant LZ25D060002 and the Fundamental Research Funds for the Central Universities under Grant 226-2025-00150. Anzhou Cao acknowledges the Funding of ZJU Tang Scholar. This study is also supported by the Ministry of Education, Culture, Sports, Science and Technology, Japan (MEXT) to a project on Joint Usage/Research Center–Leading Academia in Marine and Environment Pollution Research (Lamer).

Appendix A. Supplementary data

Supplementary data to this article can be found online at https://doi.org/10.1016/j.ecss.2026.109842.

Data availability

Data will be made available on request.

References

Amaya, D.J., Alexander, M.A., Capotondi, A., Deser, C., Karnauskas, K.B., Miller, A.J., Mantua, N.J., 2021. Are long-term changes in mixed layer depth influencing north Pacific marine heatwaves? Bull. Am. Meteorol. Soc. 102, S59–S66. https://doi.org/10.1175/BAMS-D-20-0144.1.

Amaya, D.J., Jacox, M.G., Alexander, M.A., Scott, J.D., Deser, C., Capotondi, A., Phillips, A.S., 2023. Bottom marine heatwaves along the Continental shelves of North America. Nat. Commun. 14, 1038. https://doi.org/10.1038/s41467-023-36567-0.

Anticamara, J.A., Go, K.T.B., 2017. Impacts of super-typhoon Yolanda on Philippine reefs and communities. Reg. Environ. Change 17, 703–713. https://doi.org/10.1007/s10113-016-1062-8.

Balaguru, K., Foltz, G.R., Leung, L.R., Xu, W., Kim, D., Lopez, H., West, R., 2022. Increasing hurricane intensification rate near the US Atlantic coast. Geophys. Res. Lett. 49. https://doi.org/10.1029/2022GL099793 e2022GL099793.

Bian, C., Jing, Z., Wang, H., Wu, L., Chen, Z., Gan, B., Yang, H., 2023. Oceanic mesoscale eddies as crucial drivers of global marine heatwaves. Nat. Commun. 14, 2970. https://doi.org/10.1038/s41467-023-38811-z.

Bond, N.A., Cronin, M.F., Freeland, H., Mantua, N., 2015. Causes and impacts of the 2014 warm anomaly in the NE Pacific. Geophys. Res. Lett. 42, 3414–3420. https://doi.org/10.1002/2015GL063306.

Cao, A., Guo, Z., Song, J., Lv, X., He, H., Fan, W., 2018. Near-inertial waves and their underlying mechanisms based on the South China Sea internal wave experiment (2010-2011). J. Geophys. Res. Ocean. 123, 5026–5040. https://doi.org/10.1029/2018JC013753.

Capotondi, A., Rodrigues, R.R., Sen Gupta, A., Benthuysen, J.A., Deser, C., Frölicher, T. L., Lovenduski, N.S., Amaya, D.J., Grix, N.L., Xu, T., Hermes, J., Holbrook, N.J., Martinez-Villalobos, C., Masina, S., Roxy, M.K., Schaeffer, A., Schlegel, R.S., Smith, K.E., Wang, C., 2024. A global overview of marine heatwaves in a changing climate. Commun. Earth Environ. 5, 701. https://doi.org/10.1038/s43247-024-01806-9.

Cheng, L., Zhu, J., Abraham, J., Trenberth, K.E., Fasullo, J.T., Zhang, B., Yu, F., Wan, L., Chen, X., Song, X., 2019. 2018 continues record global ocean warming. Adv. Atmos. Sci. 36, 249–252. https://doi.org/10.1007/s00376-019-8276-x.

Cheng, L., Zhu, J., Sriver, R.L., 2015. Global representation of tropical cyclone-induced short-term ocean thermal changes using Argo data. Ocean Sci. 11, 719–741. https://doi.org/10.5194/os-11-719-2015.

Cheng, S., Cao, A., Song, J., Guo, X., 2024. Contribution of high-mode near-inertial waves to enhanced typhoon-induced sea surface temperature cooling in the South China Sea. Ocean Model. 192, 102452. https://doi.org/10.1016/j.ocemod.2024.102452.

Dmitrenko, I.A., Kirillov, S.A., Bloshkina, E., Lenn, Y.D., 2012. Tide-induced vertical mixing in the Laptev Sea coastal polynya. J. Geophys. Res., Oceans 117, C09023. https://doi.org/10.1029/2011JC006966.

Dzwonkowski, B., Coogan, J., Fournier, S., Lockridge, G., Park, K., Lee, T., 2020. Compounding impact of severe weather events fuels marine heatwave in the coastal ocean. Nat. Commun. 11, 4623. https://doi.org/10.1038/s41467-020-18339-2.

Emanuel, K., 2001. Contribution of tropical cyclones to meridional heat transport by the oceans. J. Geophys. Res. Atmos. 106, 14771–14781. https://doi.org/10.1029/2000JD900641.

Emanuel, K., 2005. Increasing destructiveness of tropical cyclones over the past 30 years. Nature 436, 686–688. https://doi.org/10.1038/nature03906.

Frölicher, T.L., Fischer, E.M., Gruber, N., 2018. Marine heatwaves under global warming. Nature 560, 360–364. https://doi.org/10.1038/s41586-018-0383-9.

Frölicher, T.L., Laufkötter, C., 2018. Emerging risks from marine heat waves. Nat. Commun. 9, 650. https://doi.org/10.1038/s41467-018-03163-6.

Gruber, N., Boyd, P.W., Frölicher, T.L., Vogt, M., 2021. Biogeochemical extremes and compound events in the ocean. Nature 600, 395–407. https://doi.org/10.1038/s41586-021-03981-7.

Guibourd de Luzinais, V., Gascuel, D., Reygondeau, G., Cheung, W.W., 2024. Large potential impacts of marine heatwaves on ecosystem functioning. Glob. Chang. Biol. 30, e17437. https://doi.org/10.1111/gcb.17437.

Guo, X., Gao, Y., Zhang, S., Cai, W., Chen, D., Leung, L.R., Zscheischler, J., Thompson, L., Davis, K., Qu, B., Gao, H., Wu, L., 2024. Intensification of future subsurface marine heatwaves in an eddy-resolving model. Nat. Commun. 15, 10777. https://doi.org/10.1038/s41467-024-54946-z.

Han, C., Bowen, M., Sutton, P., 2024. The response of the upper ocean to tropical cyclones in the South Pacific. J. Geophys. Res., Oceans 129. https://doi.org/10.1029/2023JC020627 e2023JC020627.

He, Q., Zhan, W., Feng, M., Gong, Y., Cai, S., Zhan, H., 2024. Common occurrences of subsurface heatwaves and cold spells in ocean eddies. Nature 634, 1111–1117. https://doi.org/10.1038/s41586-024-08051-2.

He, H.L., Chen, D.K., 2011. Effects of surface wave breaking on the oceanic boundary layer. Geophys. Res. Lett. 38 (7), L07604. https://doi.org/10.1029/2011GL046665.

Hobday, A.J., Alexander, L.V., Perkins, S.E., Smale, D.A., Straub, S.C., Oliver, E.C.J., Benthuysen, J.A., Burrows, M.T., Donat, M.G., Feng, M., Holbrook, N.J., Moore, P.J., Scannell, H.A., Sen Gupta, A., Wernberg, T., 2016. A hierarchical approach to defining marine heatwaves. Prog. Oceanogr. 141, 227–238. https://doi.org/10.1016/j.pocean.2015.12.014.

Holbrook, N.J., Scannell, H.A., Sen Gupta, A., Benthuysen, J.A., Feng, M., Oliver, E.C., Alexander, L.V., Burrows, M.T., Donat, M.G., Hobday, A.J., Moore, P.J., Perkins-Kirkpatrick, S.E., Smale, D.A., Straub, S.C., Wernberg, T., 2019. A global assessment of marine heatwaves and their drivers. Nat. Commun. 10, 2624. https://doi.org/10.1038/s41467-019-10206-z.

Hongo, C., Kawamata, H., Goto, K., 2012. Catastrophic impact of typhoon waves on coral communities in the Ryukyu Islands under global warming. J. Geophys. Res. Biogeosci. 117. https://doi.org/10.1029/2011JG001902.

Hsu, P.C., Ho, C.R., 2019. Typhoon-induced ocean subsurface variations from glider data in the Kuroshio region adjacent to Taiwan. J. Oceanogr. 75, 1–21. https://doi.org/10.1007/s10872-018-0480-2.

Hu, S., Li, S., Zhang, Y., Guan, C., Du, Y., Feng, M., Ando, K., Wang, F., Schiller, A., Hu, D., 2021. Observed strong subsurface marine heatwaves in the tropical western Pacific Ocean. Environ. Res. Lett. 16, 104024. https://doi.org/10.1088/1748-9326/ac26f2.

IPCC, 2021. In: Masson-Delmotte, V., Zhai, P., Pirani, A., Connors, S.L., Péan, C., Berger, S., Caud, N., Chen, Y., Goldfarb, L., Gomis, M.I., Huang, M., Leitzell, K., Lonnoy, E., Matthews, J.B.R., Maycock, T.K., Waterfield, T., Yelekçi, O., Yu, R., Zhou, B. (Eds.), Climate Change 2021: the Physical Science Basis. Contribution of Working Group I to the Sixth Assessment Report of the Intergovernmental Panel on Climate Change [Core Writing Team. IPCC, Geneva, Switzerland, pp. 1211–1362. https://doi.org/10.1017/9781009157896.

IPCC, 2022. Climate Change 2022: impacts, adaptation, and Vulnerability. In: Pörtner, H.-O., Roberts, D.C., Tignor, M., Poloczanska, E.S., Mintenbeck, K., Alegría, A., Craig, M., Langsdorf, S., Löschke, S., Möller, V., Okem, A., Rama, B. (Eds.), Contribution of Working Group II to the Sixth Assessment Report of the Intergovernmental Panel on Climate Change [Core Writing Team. IPCC, Geneva, Switzerland, p. 3056. https://doi.org/10.1017/9781009325844.

Jacob, S.D., Shay, L.K., Mariano, A.J., Black, P.G., 2000. The 3D oceanic mixed layer response to Hurricane Gilbert. J. Phys. Oceanogr. 30, 1407–1429. https://doi.org/10.1175/1520-0485(2000)030%3C1407:TOMLRT%3E2.0.CO;2.

Jean-Michel, L., Eric, G., Romain, Bé-B., Gilles, G., Angélique, M., Marie, D., Clément, B., Mathieu, H., Olivier, L.G., Charly, R., Tony, C., Charles-Emmanuel, T., Florent, G., Giovanni, R., Mounir, B., Yann, D., Pierre-Yves, L.T., 2021. The copernicus global 1/12 oceanic and sea ice GLORYS12 reanalysis. Front. Earth Sci. 9, 698876. https://doi.org/10.3389/feart.2021.698876.

Köhn, E.E., Vogt, M., Münnich, M., Gruber, N., 2024. On the vertical structure and propagation of marine heatwaves in the Eastern Pacific. J. Geophys. Res., Oceans 129. https://doi.org/10.1029/2023JC020063 e2023JC020063.

Li, Q., Fu, G., Guo, J., Yang, Y., Duan, Y., 2005. An observational study of typhoon Imbudo in 2003. J. Ocean Univ. China 4, 391–397. https://doi.org/10.1007/s11802-005-0061-z.

Lin, I.I., Wu, C.C., Pun, I.F., Ko, D.S., 2008. Upper-ocean thermal structure and the western North Pacific category 5 typhoons. Part I: ocean features and the category 5 typhoons' intensification. Mon. Weather Rev. 136, 3288–3306. https://doi.org/10.1175/2008MWR2277.1.

Liu, X., Zhai, F., Yan, J., Gu, Y., Wang, Y., Li, P., Wu, K., 2022. Three-dimensional temperature responses to northward-moving typhoons in the shallow stratified Yellow Sea in summer. J. Geophys. Res., Oceans 127. https://doi.org/10.1029/2022JC019091 e2022JC019091.

Liu, Y., Guan, S., Lin, I.-I., Mei, W., Jin, F.-F., Huang, M., Zhang, Y., Zhao, W., Tian, J., 2023. Effect of storm size on sea surface cooling and tropical cyclone intensification in the Western North Pacific. J. Clim. 36 (20), 7277–7296. https://doi.org/10.1175/JCLI-D-22-0949.1.

Liu, Z., Jiao, L., Lian, X., 2025. Changes in compound extreme events and their impacts on cropland productivity in China, 1985-2019. Earths Future 13. https://doi.org/10.1029/2024EF005038 e2024EF005038.

Long, J., Giri, C., Primavera, J., Trivedi, M., 2016. Damage and recovery assessment of the Philippines' mangroves following Super Typhoon Haiyan. Mar. Pollut. Bull. 109, 734–743. https://doi.org/10.1016/j.marpolbul.2016.06.080.

Lu, X., Yu, H., Ying, M., Zhao, B., Zhang, S., Lin, L., Bai, L., Wan, R., 2021. Western North Pacific tropical cyclone database created by the China Meteorological

Administration. Adv. Atmos. Sci. 38, 690–699. https://doi.org/10.1007/s00376-020-0211-7.
Monterey, G.I., Levitus, S., 1997. Seasonal variability of mixed layer depth for the world ocean. NOAA Atlas NESDIS 14, 2. U.S. Dep. of Comm. Washington, DC.
Muis, S., Verlaan, M., Winsemius, H.C., Aerts, J.C., Ward, P.J., 2016. A global reanalysis of storm surges and extreme sea levels. Nat. Commun. 7, 11969. https://doi.org/10.1038/ncomms11969.
Oliver, E.C., Donat, M.G., Burrows, M.T., Moore, P.J., Smale, D.A., Alexander, L.V., Benthuysen, J.A., Feng, M., Sen Gupta, A., Hobday, A.J., Holbrook, N.J., Perkins-Kirkpatrick, S.E., Scannell, H.A., Straub, S.C., Wernberg, T., 2018. Longer and more frequent marine heatwaves over the past century. Nat. Commun. 9, 1324. https://doi.org/10.1038/s41467-018-03732-9.
Park, J.J., Kwon, Y.O., Price, J.F., 2011. Argo array observation of ocean heat content changes induced by tropical cyclones in the north Pacific. J. Geophys. Res., Oceans 116. https://doi.org/10.1029/2011JC007165.
Pearce, A.F., Feng, M., 2013. The rise and fall of the "marine heat wave" off Western Australia during the summer of 2010/2011. J. Mar. Syst. 111, 139–156. https://doi.org/10.1016/j.jmarsys.2012.10.009.
Pei, Y., Zhang, R., Chen, D., 2015. Upper ocean response to tropical cyclone wind forcing: a case study of typhoon rammasun (2008). Sci. China Earth Sci. 58, 1623–1632. https://doi.org/10.1007/s11430-015-5127-1.
Polton, J.A., Smith, J.A., Mackinnon, J.A., Tejada-Martínez, A.E., 2008. Rapid generation of high-frequency internal waves beneath a wind and wave forced oceanic surface mixed layer. Geophys. Res. Lett. 35 (13), L13602. https://doi.org/10.1029/2008GL033856.
Price, J.F., 1981. Upper ocean response to a hurricane. J. Phys. Oceanogr. 11, 153–175. https://doi.org/10.1175/1520-0485(1981)011%3C0153:UORTAH%3E2.0.CO;2.
Pun, I.F., Lin, I.I., Wu, C.C., 2025. Suppression of marine heatwave activity by tropical cyclone-induced upper ocean cooling. Sci. Adv. 11 (eadw8070). https://doi.org/10.1126/sciadv.adw8070.
Pun, I.I., Lin, C., Lien, C., Wu, C., 2018. Influence of the size of super typhoon megi (2010) on SST cooling. Mon. Weather Rev. 146 (3), 661–677. https://doi.org/10.1175/MWR-D-17-0044.1.
Qiao, M., Cao, A., Song, J., Pan, Y., He, H., 2022. Enhanced turbulent mixing in the upper ocean induced by super typhoon goni (2015). Remote Sens. 14, 2300. https://doi.org/10.3390/rs14102300.
Raja, K.J., Buijsman, M.C., Shriver, J.F., Arbic, B.K., Siyanbola, O., 2022. Near-inertial wave energetics modulated by background flows in a global model simulation. J. Phys. Oceanogr. 52, 823–840. https://doi.org/10.1175/JPO-D-21-0130.1.
Schaeffer, A., Sen Gupta, A., Roughan, M., 2023. Seasonal stratification and complex local dynamics control the sub-surface structure of marine heatwaves in eastern Australian coastal waters. Commun. Earth Environ. 4, 304. https://doi.org/10.1038/s43247-023-00966-4.
Schaeffer, A., Roughan, M., 2017. Subsurface intensification of marine heatwaves off southeastern Australia: the role of stratification and local winds. Geophys. Res. Lett. 44, 5025–5033. https://doi.org/10.1002/2017GL073714.
Smale, D.A., Wernberg, T., Oliver, E.C., Thomsen, M., Harvey, B.P., Straub, S.C., Burrows, M.T., Alexander, L.V., Benthuysen, J.A., Donat, M.G., Feng, M., Hobday, A. J., Holbrook, N.J., Perkins-Kirkpatrick, S.E., Scannell, H.A., Sen Gupta, A., Payne, B. L., Moore, P.J., 2019. Marine heatwaves threaten global biodiversity and the provision of ecosystem services. Nat. Clim. Chang. 9, 306–312. https://doi.org/10.1038/s41558-019-0412-1.
Sun, D., Li, F., Jing, Z., Hu, S., Zhang, B., 2023. Frequent marine heatwaves hidden below the surface of the global ocean. Nat. Geosci. 16, 1099–1104. https://doi.org/10.1038/s41561-023-01325-w.
Thomson, J.A., Burkholder, D.A., Heithaus, M.R., Fourqurean, J.W., Fraser, M.W., Statton, J., Kendrick, G.A., 2014. Extreme temperatures, foundation species, and abrupt ecosystem change: an example from an iconic seagrass ecosystem. Glob. Chang. Biol. 21, 1463–1474. https://doi.org/10.1111/gcb.12694.
Vincent, E.M., Madec, G., Lengaigne, M., Vialard, J., Koch-Larrouy, A., 2013. Influence of tropical cyclones on sea surface temperature seasonal cycle and ocean heat transport. Climate Dyn 41, 2019–2038. https://doi.org/10.1007/s00382-012-1556-0.
Wernberg, T., Smale, D.A., Tuya, F., Thomsen, M.S., Langlois, T.J., De Bettignies, T., Bennett, S., Rousseaux, C.S., 2013. An extreme climatic event alters marine ecosystem structure in a global biodiversity hotspot. Nat. Clim. Chang. 3, 78–82. https://doi.org/10.1038/nclimate1627.
Ying, M., Zhang, W., Yu, H., Lu, X., Feng, J., Fan, Y., Zhu, Y., Chen, D., 2014. An overview of the China meteorological administration tropical cyclone database. J. Atmos. Oceanic Technol. 31, 287–301. https://doi.org/10.1175/JTECH-D-12-00119.1.
Zhang, H., 2023. Modulation of upper ocean vertical temperature structure and heat content by a fast-moving tropical cyclone. J. Phys. Oceanogr. 53, 493–508. https://doi.org/10.1175/JPO-D-22-0132.1.
Zhang, H., Chen, D., Zhou, L., Liu, X., Ding, T., Zhou, B., 2016. Upper ocean response to typhoon kalmaegi (2014). J. Geophys. Res., Oceans 121, 6520–6535. https://doi.org/10.1002/2016JC012064.
Zhang, H., He, H., Zhang, W.Z., Tian, D., 2021. Upper ocean response to tropical cyclones: a review. Geosci. Lett. 8, 1–12. https://doi.org/10.1186/s40562-020-00170-8.
Zhang, W., Li, R., Zhu, D., Zhao, D., Guan, C., 2023a. An investigation of impacts of surface waves-induced mixing on the upper ocean under typhoon megi (2010). Remote Sens. 15, 1862. https://doi.org/10.3390/rs15071862.
Zhang, Y., Du, Y., Feng, M., Hobday, A.J., 2023b. Vertical structures of marine heatwaves. Nat. Commun. 14, 6483. https://doi.org/10.1038/s41467-023-42219-0.
Zhang, Y., Zhang, H., Tang, X., Yang, S., Wang, Y., Lin, X., Tian, D., Chen, D., 2024. Oceanic response to tropical cyclone in the northern South China Sea observed by underwater gliders during 2018 and 2020. Deep-Sea Res., Part A I 213, 104387. https://doi.org/10.1016/j.dsr.2024.104387.
Zhao, B., Qiao, F., Cavaleri, L., Wang, G., Bertotti, L., Liu, L., 2017. Sensitivity of typhoon modeling to surface waves and rainfall. J. Geophys. Res., Oceans 122, 1702–1723. https://doi.org/10.1002/2016JC012262.
Zhao, Z., Marin, M., 2019. A MATLAB toolbox to detect and analyze marine heatwaves. J. Open Source Softw. 4, 1124. https://doi.org/10.21105/joss.01124.
Zhou, X., Xu, K., Ashok, K., Shi, J., Zhang, L., Lu, J.Y., Liu, B., Tam, C.Y., Xu, H., Wang, W., 2025. Compound marine heatwaves and tropical cyclones delay the onset of the Bay of Bengal summer monsoon. npj Clim. Atmos. Sci. 8, 162. https://doi.org/10.1038/s41612-025-01061-5.
Zscheischler, J., Westra, S., Van Den Hurk, B.J., Seneviratne, S.I., Ward, P.J., Pitman, A., AghaKouchak, A., Bresch, D.N., Leonard, M., Wahl, T., Zhang, X., 2018. Future climate risk from compound events. Nat. Clim. Chang. 8, 469–477. https://doi.org/10.1038/s41558-018-0156-3.
Zscheischler, J., Seneviratne, S.I., 2017. Dependence of drivers affects risks associated with compound events. Sci. Adv. 3, e1700263. https://doi.org/10.1126/sciadv.1700263.